

Giant magnetoresistance in Fe/Ag multilayers and its anomalous temperature dependence

Chengtao Yu, Shuxiang Li, Wuyan Lai, Minglang Yan, Yizhong Wang, and
Zhenxi Wang

*State Key Laboratory for Magnetism, Institute of Physics, Chinese Academy of Sciences,
P.O. Box 603, Beijing 100080, China*

(Received 6 July 1994; revised manuscript received 20 January 1995)

The observation of giant magnetoresistance (GMR) effect in sputtered Fe/Ag multilayers is presented. The observed maximum GMR amounts to -7.3% at 1.5 K. The amplitude of the GMR oscillates with variation of Ag thickness, and the oscillation period is about 11 Å. The origin of the GMR in these Fe/Ag multilayers is believed to lie mainly in the interface. The GMR effect contains contributions either arising from the antiferromagnetic coupled magnetization in the neighboring Fe layer or superparamagneticlike spins at the interface. An anomalous temperature dependence of magnetoresistance is reported and it is attributed to the suppression of thermal excitations of superparamagneticlike spins by applied magnetic field, which results in a reduction of the GMR effect with decreasing temperature. In addition, the specific field dependence of the magnetoresistance curve with respect to temperature is also accounted for by the contribution from those arising from superparamagneticlike spins at the interface, which could be easily quenched at low temperature, leading to the observation of a decreasing tendency of saturation field with decreasing temperature.

I. INTRODUCTION

Since Baibich *et al.*¹ found giant magnetoresistance (GMR) in antiferromagnetic coupled Fe/Cr multilayers in 1988, extensive research has been done concerning both interlayer coupling and magnetoresistance in various magnetic/nonmagnetic metal multilayers. It was then found that in a number of magnetic multilayers including Fe/Cr, Co/Cr, Co/Ru,² Fe/Cu,³ and Co/Cu (Ref. 4) to name just a few, an oscillatory GMR as function of nonmagnetic spacer thickness is present and it is coherently associated with interlayer coupling oscillation between ferromagnetic (FM) and antiferromagnetic (AFM) coupling. The nature of the coupling is generally thought of as arising from the spin polarization of the conduction electrons in the spacer layer adjacent to the magnetic layer. A variety of different approaches have been employed to model the coupling, but they are often compared to Ruderman-Kittel-Kasuya-Yosida (RKKY)-like behavior with the result dependent upon the Fermi surface of the spacer material.^{5,6} On the other hand, a coherent interplay of spin-dependent scattering of the conduction electrons occurring in the magnetic layer or at the interface based on the two current model⁷ is supposed to be at the origin of the GMR. This spin-dependent scattering is directly related to the asymmetry of the unfilled *d*-band structure in the ferromagnetic layers, and the magnetoresistance is just a result of antiparallel arrangements of magnetization between neighboring magnetic layers. Theoretical understanding of the GMR has been made by either a semiclassical approach⁸ based on the Boltzmann equation and Fuchs-Sondheimer theory for size effects in electronic transport or a quantum-statistical method⁹ based on Kubo formalism. Besides the multi-

layer geometry, in granular films which consist of ultrafine magnetic particles embedded in noble metallic matrix, giant magnetoresistance has also been reported,¹⁰ and now it originates from spin-dependent scattering by randomly aligned single-domain regions. In early work about Fe/Ag trilayer, antiferromagnetic coupling was not observed,¹¹ but theoretical calculation based on the RKKY-like model on transition magnetic metal/noble metal multilayers⁶ predicted that there exists interlayer coupling oscillation between ferromagnetic and antiferromagnetic coupling, with the oscillation period being determined by the topologic properties of the spacer Fermi surface, more precisely by the wave vectors that are perpendicular to the interface and span nearly parallel parts of the Fermi surface. More recently, in molecular-beam-epitaxy (MBE) grown Fe(100)/Ag/Fe trilayers at an elevated substrate temperature,^{12,13} an oscillatory behavior of interlayer coupling has been found, and both bilinear and biquadratic exchange coupling have been observed. Furthermore, in FeAg granular films, an apparent GMR effect is present.¹⁴ This implies the presence of strong spin-dependent electron scattering in the Fe/Ag system. However, to the best of our knowledge, no observation of giant magnetoresistance has been reported in Fe/Ag multilayers. In this paper, the observation of giant magnetoresistance in sputtered Fe/Ag multilayers is presented. It was found that the GMR oscillates with variation of Ag thickness and the oscillation period is about 11 Å. The GMR observed here is believed to be attributable to spin-dependent scattering mainly occurring at the interface. An anomalous temperature dependence of both the GMR and saturation field is also reported, which is very different from what the GMR is just at the origin of spin-dependent scattering based on antiferromagnetic

coupling between neighboring magnetic layers. Both unusual temperature dependences have been interpreted in the light of thermal excitation of interfacial superparamagnetic spins.

This paper is organized as follows: In Sec. II we describe the experimental method. Section III contains the main results about structural, magnetotransport, and magnetic properties. In Sec. IV A, extensive discussion about the origin of the GMR in our Fe/Ag multilayers is presented. Section IV B provides an explanation of the oscillatory GMR by considering the influence of interface roughness. In Sec. IV C the anomalous temperature dependence of saturation field is discussed, and in Sec. IV D explanation about the temperature dependence of the GMR is given. Finally, Sec. V summarizes the main observations and conclusions of the work.

II. EXPERIMENTAL METHOD

The Fe/Ag multilayers for these studies were deposited onto water-cooled silicon substrates by dc-magnetron sputtering in argon plasma of 0.5 Pa after a base pressure better than 3×10^{-5} Pa had been achieved. A SiO₂ buffer layer with thickness 80 Å was deposited before depositing the Fe and Ag layers. The deposition rate for Fe and Ag was 0.9 Å/sec and 0.8 Å/sec, respectively. A series of up to eight samples with different superstructures were produced at a time without breaking vacuum, and the thickness of a single layer for both Fe and Ag was adjusted by controlling deposition time via computerized control of the shutter and rotation of the substrate platform. A typical Fe/Ag multilayer sample was given by the following structure: silicon/SiO₂(80 Å)/[Fe(10 Å)/Ag(t_{Ag})]₄₀, where the single Fe layer was fixed to 10 Å, the Ag layer thickness t_{Ag} varied in a wide range, and the number of the bilayers was 40. The periodic superstructure of Fe/Ag multilayers was examined by low-angle x-ray diffraction on a Demax-RB system using Cu $K\alpha$ radiation and also by cross-sectional transmission electron microscopy (XTEM). A standard four-point probe method was employed to measure the magnetoresistance (MR) with magnetic field applied in the film plane but perpendicular to sensing current. The magnetoresistance was calculated in terms of $[(\rho_H - \rho)/\rho] \times 100\%$, where ρ and ρ_H represent the nonfield resistivity and the resistivity at external field H , respectively. Measurements of magnetization loops were performed on a vibrating sample magnetometer with a maximum applied field of 30 kOe and a moment resolution of better than 5×10^{-6} emu.

III. RESULTS

Figure 1 shows the low-angle x-ray-diffraction patterns for three representative samples [Fe(10 Å)/Ag(t_{Ag})]₄₀ with $t_{Ag} = 10, 21, \text{ and } 32$ Å, respectively. As seen in this figure, Bragg diffraction peaks up to the third order appear, and it is indicative of the existence of a superlattice structure. It is worth noting that with increasing t_{Ag} , the diffraction patterns undergo apparent evolution. For sample with $t_{Ag} = 10$ Å, only the first-order

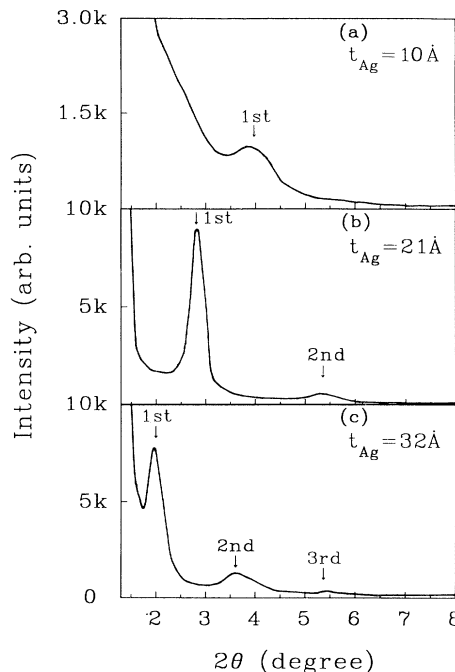


FIG. 1. The low-angle x-ray-diffraction patterns for samples [Fe(10 Å)/Ag(t_{Ag})]₄₀ with t_{Ag} about (a) 10 Å, (b) 21 Å, and (c) 32 Å.

peak is present, and it is very dull with wide full width at half maximum (FWHM), indicating the presence of significant interfacial roughness. This roughness may be caused by disorder in the layer thickness, which could destroy the long-range order, resulting in peak broadening as well as damping of high-order peak intensity.¹⁵ But for a thicker Ag spacer, the situation changes considerably. When $t_{Ag} = 32$ Å, the third-order peak is visible on the diffraction spectrum and it also shows sharper peaks with narrower FWHM. These imply significant improvement of the superstructure.

The superstructure has also been investigated by high-angle x-ray diffraction. The high-angle x-ray-diffraction patterns for the same samples are shown in Fig. 2. As can be seen, several additional superlattice peaks are visible, which is a confirmation of the clear composition modulation of the film. The high intensity Bragg peak between Ag(111) and Fe(110) suggests a predominant texture with Ag(111) and Fe(110) orientation on the film growth direction, which is consistent with literature.¹⁶ For samples with thicker t_{Ag} [see Figs. 2(b) and 2(c)], except for the central Bragg peaks additional satellite peaks appear around the central peak. When $t_{Ag} = 32$ Å, four satellites are observed, indicating coherent stacking of atomic planes across Ag and Fe layers. For $t_{Ag} = 21$ Å, three satellite peaks are visible on the patterns. These satellites are strong evidence of multilayered structure. The satellite patterns exhibit obvious asymmetry in intensity, indicating the existence of interlayer mismatch.¹⁵ With increasing Ag layer thickness, the superlattice Bragg peaks shift toward lower angles. This shift, combined with quite

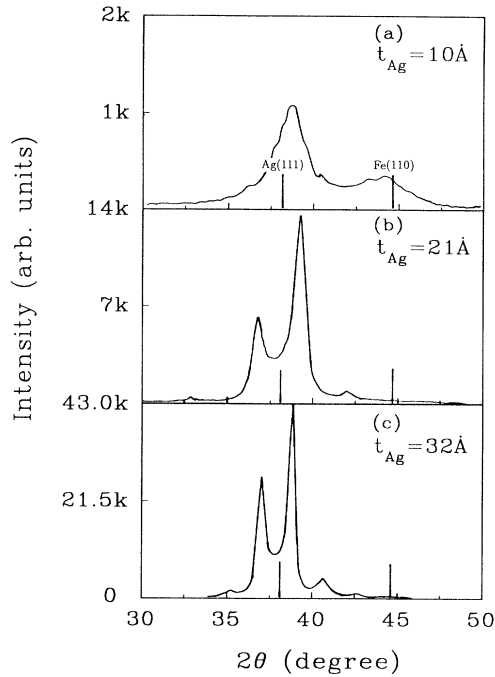


FIG. 2. The high-angle x-ray-diffraction patterns for samples $[\text{Fe}(10 \text{ \AA})/\text{Ag}(t_{\text{Ag}})]_{40}$ with t_{Ag} about (a) 10 Å, (b) 21 Å, and (c) 32 Å. The Ag(111) and Fe(110) x-ray-diffraction lines are also given on the patterns.

narrow peaks, suggests that the Fe/Ag interface is coherent in large areas. These superlattice peaks are diffraction results from the lattice according to the averaging lattice parameters of both Fe and Ag atoms. However, for the thinner sample with $t_{\text{Ag}}=10 \text{ \AA}$, the diffraction pattern seems to be somewhat different. The intensity of the Bragg peak near Ag(111) is much lower and also has wide width. Besides, no apparent satellite is observed. This may indicate a degradation of superlattice structure due to discrete growth of the layer, resulting in significant roughness. It is consistent with the low-angle x-ray-diffraction data.

The superlattice structure is also verified by XTEM. Figure 3 shows the micrograph of the same sample shown in Figs. 1(b) and 2(b). It can be seen that the sample possesses appreciable multilayered structure, but with obvious defects in their layered structure. The white layer in the image corresponds to Fe layer, and the dark layer corresponds to Ag layer. The Ag layers over the whole film are continuous, but show small variation of layer thickness. On the other hand, the Fe layers also are continuous in most of the area, but with significant defects of rumpling or even rupture. This kind of defect may be owing to an islandlike growth of the Fe layer in the initial stage and also the grain-to-grain epitaxy growth through the Ag and Fe layer. As can be seen, the microstructures are obviously characteristic of columnar crystalline grains, with the grain size several times larger than the modulation period and in the order of hundreds of angstroms. Within individual grain, both Fe and Ag layer grow fairly smooth, with an appreciable flatness of

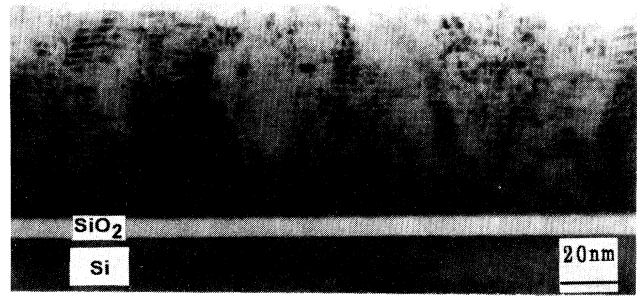


FIG. 3. The cross-section TEM image of sample $[\text{Fe}(10 \text{ \AA})/\text{Ag}(21 \text{ \AA})]_{40}$. The white layer corresponds to Fe layer, and the dark layer to Ag layer.

interface, which is attributed to an epitaxy growing of Ag and Fe through the whole columnar grain. However, these columnar grains form significant boundary grooving, to some extent, which cause the layer to bend in some locations or even to interrupt in the Fe layer, resulting in much incomplete layered structure or interface roughness.

Figure 4 shows the MR curves correlated with applied magnetic field for the same representative samples as in Fig. 1 at a temperature of 1.5 K and room temperature, respectively. As seen, at 1.5 K the MR values experience dramatic changes with increasing applied magnetic field in the initial stage, then they vary slowly and approach saturation gradually with further increas-

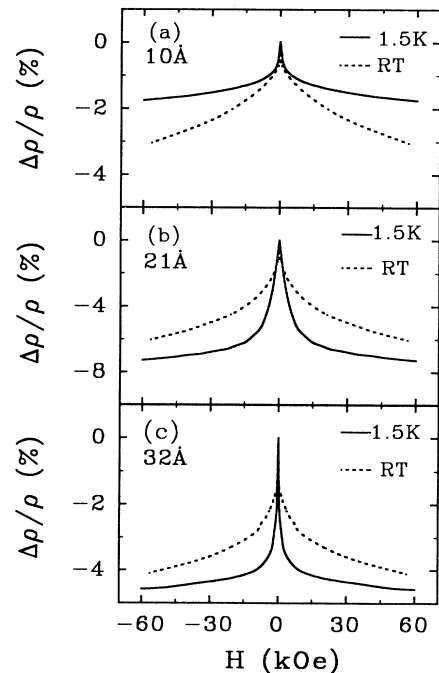


FIG. 4. The MR curves vs applied magnetic field for samples $[\text{Fe}(10 \text{ \AA})/\text{Ag}(t_{\text{Ag}})]_{40}$ with t_{Ag} about (a) 10 Å, (b) 21 Å, and (c) 32 Å at temperature 1.5 K and room temperature, respectively.

ing field, but there is no accomplishment of complete saturation. While at room temperature, the MR values change smoothly all the while and even in the maximum magnetic field available here it still shows no sign of saturation. The saturation field is unusually larger than that at low temperature. What is more unusual is that for the sample with $t_{\text{Ag}}=10 \text{ \AA}$ [Fig. 4(a)], the MR at 1.5 K is even smaller than that at room temperature. It is controversial to the general understanding that the MR increases with decreasing temperature due to a weak temperature dependence of $\Delta\rho$ and the reduction of ρ , resulting from damping phonon and magnon excitations.⁴

Figure 5 demonstrates the variation of MR as a function of Ag thickness for a series of samples $[\text{Fe}(10 \text{ \AA})/\text{Ag}(t_{\text{Ag}})]_{40}$ at temperature 1.5 K and room temperature, respectively. The MR values exhibit an oscillatory behavior with respect to t_{Ag} , and three peaks are apparent with intervals about 11 \AA , which is approximately consistent with the periodicity of interlayer coupling oscillation predicted on the Ag(111) direction by Bruno and Chappert.⁶ The amplitude of the MR for the three peaks are -3.1 , -6.1 , and -4.1% at room temperature, and -2.0 , -7.3 , and -5.0% at 1.5 K, respectively. It is worth mentioning that for samples with t_{Ag} thinner than a crucial thickness, the MR at 1.5 K is anomalously smaller than that at room temperature [also see Fig. 4(a)]. The samples displayed in Figs. 1 and 4 now lie in the first, second, and third peak points on these oscillation curves.

In order to explore the origin of the oscillatory MR in Fe/Ag, magnetic properties are extensively studied. The normalized magnetization loops for six representative samples are plotted in Fig. 6. Those plotted on the left correspond to samples with MR values on the valley points of the oscillation curve, and those plotted on the right correspond to samples with MR values on the peak points and also the same as shown in Figs. 1, 2, and 4. From these figures, at first sight, it is easy to conclude that all samples are mainly characteristic of FM coupling,

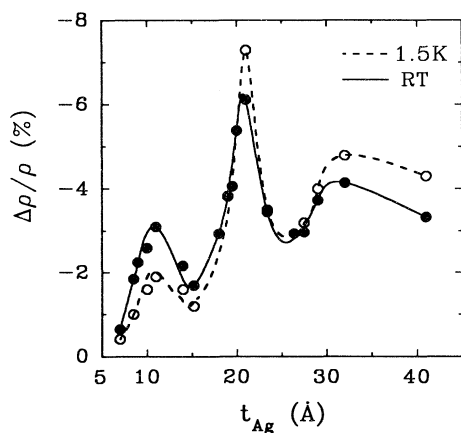


FIG. 5. Variation of MR as a function of Ag thickness t_{Ag} for samples $[\text{Fe}(10 \text{ \AA})/\text{Ag}(t_{\text{Ag}})]_{40}$ in magnetic field of 60 kOe at temperature 1.5 K and room temperature, respectively. The lines are guide to eyes.

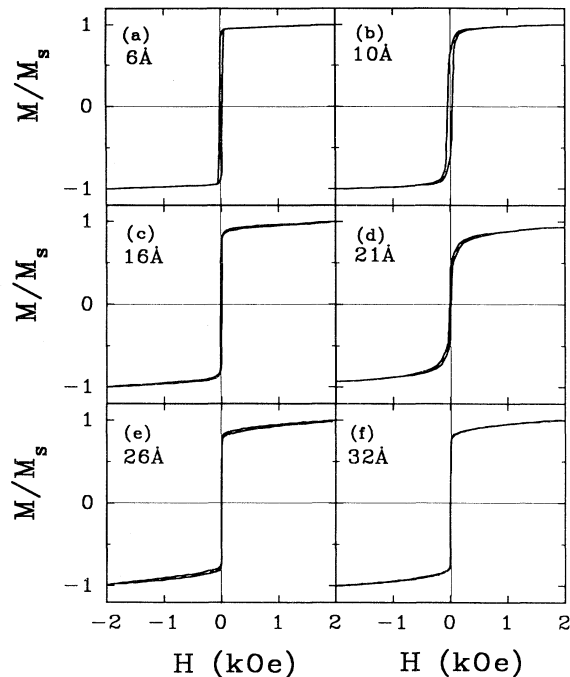


FIG. 6. Magnetization loops for samples $[\text{Fe}(10 \text{ \AA})/\text{Ag}(t_{\text{Ag}})]_{40}$ with t_{Ag} about (a) 6 \AA , (b) 10 \AA , (c) 16 \AA , (d) 21 \AA , (e) 26 \AA , and (f) 32 \AA . The magnetic field is applied parallel to the film plane.

but it should be noticed that an apparent difference exists among these loops. They differ in a manner that the magnetization curves are tilted more with smaller remanent magnetization as t_{Ag} changes from those with valley points of MR to that with peaked MR values. This implies the presence of variation of the magnetic state in neighboring magnetic Fe layers with respect to Ag thickness. As shown in this figure, for $t_{\text{Ag}}=16 \text{ \AA}$ [see Fig. 6(c)], the magnetization curve shows typical characteristics of ferromagnetic coupled multilayers with a remanent magnetization ratio more than 0.83, while for $t_{\text{Ag}}=21 \text{ \AA}$ [see Fig. 6(d)], it becomes harder to saturate the magnetization, the curve titles more with the remanent magnetization ratio decreasing to less than 0.45. This presumably is because of the presence of AFM coupling. However, with respect to variation of t_{Ag} , no complete AFM magnetization loops have been observed. The absence of complete AFM coupling between magnetic layers are different from that in sputtered Co/Ru (Ref. 2) and Fe/Cr superlattices,¹⁷ where the magnetization loops exhibit obvious alternation of AFM and FM coupling with variation of nonmagnetic thickness. However, it is similar to what observed in sputtered Co/Cu multilayers.^{18,19}

IV. DISCUSSION

A. The nature of the magnetoresistance in Fe/Ag

It has generally been accepted that the change from a configuration of antiparallel magnetization to a con-

figuration of parallel magnetization in an applied field is at the origin of the GMR in multilayer. This can be understood well on the basis of spin-dependent scattering by local magnetic moments occurring in the bulk of each magnetic layers or at interface between magnetic and nonmagnetic layer. But there is much evidence^{20–23} that the origin of the GMR lies in spin-dependent scattering from magnetic states predominantly localized at the magnetic/nonmagnetic interface. In our Fe/Ag multilayers, however, the situation seems to be more complicated, because an assemblage of superparamagneticlike spins probably arises at the interface between the Fe and Ag layer. As a result, the observed magnetoresistance effect not only depends on the general mechanism mentioned above but also closely associates with the superparamagneticlike states at the interface.

The oscillatory behavior of the GMR (see Fig. 5) can be understood in terms of the conventional spin-dependent scattering mechanism based on AFM coupling between neighboring magnetic layers. Actually, an oscillatory AFM coupling is present in these Fe/Ag multilayers though it may be weak due to the presence of multilayered structural defects. As seen in Fig. 6, with varying Ag thickness, the magnetization loops undergo appreciable changes in a way that the remanent magnetization and saturation field experience regular changes, indicative of variation of the magnetic states between neighboring Fe layers. For samples with t_{Ag} about 6, 16, and 26 Å, of which the MR values lie at the valley points, the magnetization loops [Figs. 6(a,c,e)] are mainly in character of FM coupling with much high remanent magnetization. But for samples with t_{Ag} about 10, 21, and 32 Å, which have the peaked MR values, they possess much lower remanent magnetization and also a more apparent high-field saturation behavior. These indicate that there exists AFM coupling. The correspondence between the oscillatory behavior of the GMR and the variation of the magnetic state in neighboring Fe layers is just direct evidence that the GMR effect is closely related to the AFM coupling between adjacent Fe layers. However, even for samples with the maximum GMR, only a fraction of AFM coupling is present, which coexists with a large fraction of FM coupling. This coexistence is supposed to be at the origin of the presence of local thinning of the Ag layer, pinholes or other spatial fluctuation.¹⁸ These have been confirmed by the micrograph study shown in Fig. 3. The columnar grain structure with the existence of boundary grooving provides a good condition for the occurrence of both AFM and FM coupling in a way of multidomain structure. Models about the configuration of FM and AFM domains have been proposed.¹⁹ The fraction of AFM coupling is certainly responsible for the GMR, while the observed FM coupling component is impedimental to the occurrence of the GMR. By comparing Figs. 6(b) and (d), which correspond to the first and second MR peak, respectively, one can find that the later exhibits relatively lower remanent magnetization. It is indicative of the existence of a larger fraction of AFM coupling. As a result, the maximum GMR observed just lies at the second peak rather than the first peak. The deep origin of this may lie in the imperfection of the su-

perlattice, which will be dealt with in the next section.

Although the antiferromagnetic state between the neighboring Fe layers plays an important role in the GMR effect, it seems to be not a unique role. As seen in Fig. 4, the MR curves display a specific field dependence of magnetoresistance with unusually large saturation field (H_s). It cannot be understood in a simple mechanism that the GMR is only at the origin of AFM coupling between neighboring Fe layers. Note the curves at room temperature, the magnetoresistance changes slowly in general with respect to applied magnetic field all the while, and even in the maximum field of 60 kOe, no saturation is accomplished. The saturation field is surprisingly high. In a simple model,¹⁷ where the influence of anisotropy is neglected, the interlayer coupling constant J bears a linear relationship with saturation field H_s ,

$$J = M_s t_M H_s / 4, \quad (1)$$

where M_s is the saturation magnetization of the magnetic layer and t_M is the thickness of the magnetic layer. So the interlayer coupling constant can be evaluated. Supposing the H_s was 60 kOe, the interlayer coupling constant J for [Fe(10 Å)/Ag(21 Å)]₄₀ at room temperature would be about 2.715 erg/cm², which corresponds to a surprising interlayer coupling strength and is more than one order larger than that determined from surface magneto-optical Kerr effect (SMOKE) data on a sample of a Fe(9 Å)/Ag(10 Å)/Fe(16 Å) trilayer.¹³ This obvious inconsistency suggests that the origin of the GMR in these Fe/Ag multilayers may not solely lie in a simple antiparallel arrangement of magnetization between neighboring Fe layers. It may contain an alternative mechanism. Moreover, the apparent discrepancy between the saturation field behavior of the MR curves and the magnetization loops implies that what is responsible for the GMR and for the magnetization are very different. The magnetization loop mainly reflects the magnetic state of the bulk of the Fe layers, while the GMR effect may contain contributions from either those arising from the magnetic moments in the Fe layers or that at the interface. In reality, the specific magnetic-field dependence of magnetoresistance (see Fig. 4) is reminiscent of superparamagneticlike behavior.^{22,23} Then, it is suggested that scattering from an assemblage of superparamagnetic spins, most likely at interface, is also responsible for the GMR effect. Because of the superparamagneticlike feature, it is difficult to align the moments in one orientation, so the MR curve shows a specific field dependence with a surprisingly high saturation field. In sputtered NiFe/Cu films²⁴ and even in a MBE grown Co/Cu superlattice,²³ an interfacial layer in character of superparamagnetism is present. An interfacial “loose” spin model²⁵ has also been proposed in an attempt to explain the nature of the strong temperature dependence of biquadratic coupling terms, which have been experimentally observed in Fe/Ag trilayers.^{12,13} In this model, it was postulated that localized spins at interface are weakly exchange coupled through the polarizability of the conduction band. These spins are described as dilute magnetic impurities or clusters of Fe atoms adjacent to the spacer. These inter-

facial superparamagneticlike spins are probably a result of local intermixing of Fe and Ag atoms at the interface during deposition of bombardment atoms or arising from interfacial defects. As can be seen from Fig. 3, owing to the considerable waviness and rumpling or even rupture of the Fe layer, caused by columnar grain-boundary grooving, the interface is rather rougher. Then, it is reasonable to suggest that these structure defects in the interface may accommodate some alienated spins. These spins are pinned at low temperature by the local random field, which is induced by local structural defects and stress. However, as temperature is enhanced, they may be thermally excited by overcoming the pinning energy barrier. Then, they exhibit superparamagneticlike behavior, and these spins could be called superparamagneticlike spins. The high saturation field behavior of the GMR at room temperature lies just in this origin. The superparamagneticlike behavior will be discussed further in Secs. IV C and IV D, concerning an anomalous temperature dependence of the saturation field and magnetoresistance, respectively. In addition, it should be stressed that the importance of the interfacial superparamagneticlike spins in responsibility for the GMR effect also provides evidence that spin-dependent scattering occurring at interface in these multilayers may play a dominant role in comparison with that occurring in the bulk of Fe layers. It is concluded that the GMR effect contains contributions from those either arising from AFM coupling magnetization in neighboring Fe layers or arising from superparamagneticlike spins at interface.

B. The influence of interfacial roughness

From Fig. 5, although an obvious oscillatory behavior of the GMR is present with varying t_{Ag} , the first peak is unexpectedly low. Generally, the amplitude of the GMR decays exponentially with increasing spacer thickness because of the increase of the thickness/mean free path ratio, which may result in the decoupling of the spin-dependent scattering process as predicted by theoretical models,^{8,9} and also because of the decoupling or weakening of the interlayer exchange coupling. The abnormally low MR value of the first peak may result from the imperfection of the superstructure, e.g., too much interfacial roughness. The resistivity of multilayer can be expressed as²⁶

$$\rho = \rho_0 + \rho_{s-d}(T) + \rho_M(H, T), \quad (2)$$

where the first term is the constant residual resistivity, mainly caused by defects and disorder or impurities, ρ_{s-d} includes the $s-d$ interband scattering mediated by both phonons and magnons, and ρ_M is those connected with magnetic scattering, leading to occurrence of the GMR. The interfacial roughness is believed to have direct influence on each of the terms, in particular, on ρ_M , and consequently affects the amplitude of the GMR. For the first MR peak, the Ag thickness is about 10 Å, and it lies in a region for which remarkable interfacial roughness is present. As indicated by the x-ray-diffraction patterns (see Figs. 1 and 2), for a sample with $t_{\text{Ag}}=32$ Å, several high-order satellite peaks are visible on both the

low-angle and high-angle x-ray-diffraction patterns, while $t_{\text{Ag}}=10$ Å only presents one dull Bragg peak with low intensity on the low-angle x-ray data, and no satellite peaks are visible on the high-angle pattern. This is certainly an implication of the presence of disorder in the superlattice structure or existence of significant roughness in the interface. Even in an MBE grown Fe/Ag sandwich,¹² for the first 3–4 layers of Ag the reflection high-energy electron-diffraction (RHEED) intensity oscillations are barely visible, which is an indication of significant disorder and roughness. When further grown on a Ag layer, the RHEED starts to show sharp intensity oscillation, implying improvements of surface roughness. This roughness may originate from those including intermixing disorder, mismatch strain, boundaries, and other structural or compositional disorder or defects. As can be seen from the micrograph, owing to the columnar grain grooving, the multilayer exhibits obvious roughness at the interface. It leads to a significant enhancement of resistivity ρ_0 . Thus, to some extent, it results in a lower value of $\Delta\rho/\rho$. The residual resistivity ρ_0 at 1.5 K in zero field correlated with t_{Ag} are plotted in Fig. 7. It is obvious that with reducing Ag thickness the residual resistivity increases monotonically except for the Ag thickness being at the extremely thin regime. The t_{Ag} dependence of ρ_0 can be understood by the increase of interfacial roughness as indicated by x-ray diffraction, because a rougher interface may lead to the increase of diffusive scattering at the interface and then reduces the overall mean free path of the superlattice. When the Ag spacer is extremely thin, the ρ_0 drops. This may connect with the occurrence of pinholes, leading to the increase of mean free path averaging over all layers. In addition, from Fig. 7, it is easy to conclude that the oscillatory behavior of the GMR is only due to the change in $\Delta\rho$ or ρ_M .

Besides the influence of roughness upon ρ_0 , it also have inherent influence on $\Delta\rho$ or ρ_M . The presence of roughness is generally thought to be crucial or essential for occurring GMR. In Fe/Cr (Ref. 20) and NiFe/Cu,^{21,27} it was found that a systematic increase in the interfacial roughness is enhanced the GMR. By considering three kinds of interfacial roughness including spatial geo-

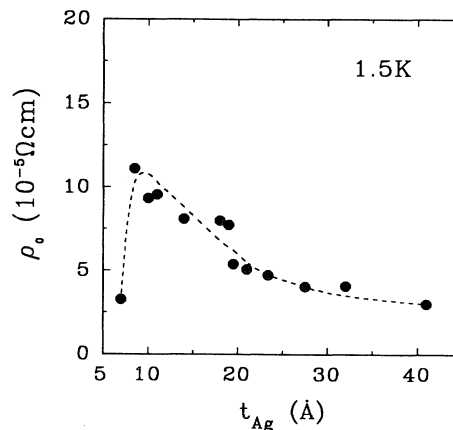


FIG. 7. The residual resistivity ρ_0 (at 1.5 K) vs Ag thickness. The dashed line is guide to eyes.

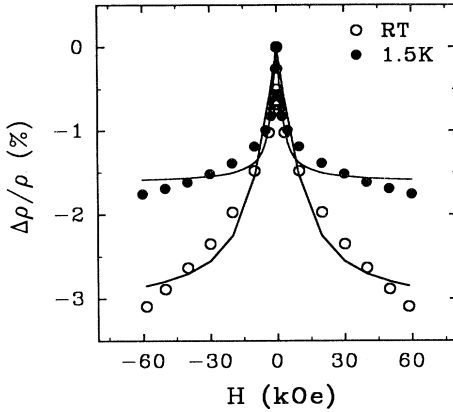


FIG. 8. The Langevin function fittings (lines) to experimental MR data for sample $[\text{Fe}(10 \text{ \AA})/\text{Ag}(10 \text{ \AA})]_{40}$ at temperature 1.5 K and room temperature, respectively.

metric roughness, correlated (quasiperiodic) roughness, and chemical (impurities or interdiffusion) roughness, Hood, Falicov, and Penn,²⁸ showed that these three aspects have complicated (not monotonical) influence on the GMR, depending on whether it increases or decreases the asymmetry in the spin-dependent scattering of the conduction electrons. For the first kind of roughness, they introduced a parameter η to describe the magnitude of the geometric roughness, their theoretical treatments demonstrated that for $0 < \eta < 2 \text{ \AA}$ the GMR undergoes dramatic changes, which may be an effect of improvement or suppression, depending upon the parameters that describe the degree of potential scattering at the interface for both majority and minority spins. But for $\eta > 2 \text{ \AA}$, the GMR generally falls off gradually. For sputtered Fe/Ag, the correlated roughness should be ruled out, and chemical-type roughness caused by interdiffusion can be neglected because of the immiscibility of Fe and Ag, so it is reasonable to consider only the geometrical roughness in an approximate approach. Thus the low MR value of the first peak may result from too much geometrical roughness, which corresponds to spatial fluctuation in the region of $\eta > 2 \text{ \AA}$. Actually, as aforementioned, the interfacial roughness for samples around the first peak, compared to samples at the second and third peaks, is surprising, but quantitative interpretation of the interfacial roughness is presently lacking.

C. The temperature dependence of saturation field of the GMR

As shown in Fig. 4, the H_s at room temperature is surprisingly larger than that at low temperature, which is very different from the fact that the GMR is mainly at origin of AFM coupling between neighboring magnetic layers. As discussed in Sec. IV A, in our Fe/Ag multilayers, besides the general term of the GMR effect, which originates from the conventional spin-dependent scattering mechanism based on AFM coupling between the neighboring Fe layers, there also exists an additional

term, which arises from spin-dependent scattering by superparamagneticlike spins at the interface. Owing to the structural defects at the interface as mentioned before, an assemblage of paramagnetic spins may be present at some location, and the local magnetic moments are weakly correlated and alienated from the bulk layer. So, they can be described as superparamagnetic spins. Based on this assumption, the saturation behavior of the GMR with respect to temperature can be understood well. At these interfacial regions the Fe atoms are present in the form of spin clusters as supposed in the “loose spin model,” and these clusters retain their magnetic moments, but they couple weakly in a way such as RKKY-type. Similar to the ultrafine magnetic particle system, at high temperature when thermal energy surpasses their indirect exchange energy, anisotropy energy as well as pinning energy induced by strain, the moments of these clusters fluctuate freely as in a paramagnetic system with each cluster bearing a great spin. Therefore, when a magnetic field is applied, it is difficult to align all the magnetic moments in one direction. So it is hard to saturate the MR as seen in Fig. 4, where no signs of saturation appear even in the maximum field available here. While the relatively low saturation fields at 1.5 K are attributed to partial freezing of the superparamagneticlike spins. As shown in Fig. 8, we have tentatively fitted the MR curves by a Langevin-like saturation function²³

$$\frac{\Delta\rho}{\rho} = -\beta \left[\coth(\alpha) - \frac{1}{\alpha} \right], \quad (3)$$

where $\alpha = N\mu_B H/k_B T$, μ_B is the Bohr magneton, k_B is the Boltzmann constant, H is the magnetic field, and T is temperature, while β and N are used as fitting parameters. It is apparent that deviations of $\Delta\rho/\rho$ from fit are quite significant. It is due to the existence of contributions originating from those rather than superparamagneticlike spins at interface. Actually, as discussed before, there exists a large portion of magnetoresistance effect just arising from the antiferromagnetic coupled magnetization. The fitting parameters β and N are temperature dependent in general, and both decrease with decreasing temperature. The reduction of N , which is in character of the size of the correlated cluster, is indicative of progressively freezing of magnetic spins at the interface. Because at 1.5 K, the low thermal energy may be unable to surpass the pinning energy, thus most of the interfacial spins lock into the bulk Fe, resulting in a comparatively low saturation field, but there still exists a long unsaturated tail, which is an implication of the presence of a small fraction of unfreezing interfacial spins. These spins may consist of a few Fe atoms or are even described as dilute Fe atoms, which are surrounded by Ag atoms. On the other hand, the reduction of β , which is a parameter in character of the maximum GMR at the saturation field, are also due to the freezing of interfacial superparamagneticlike spins, which, at high temperature, makes an extra contribution to the GMR effect. In summary, the unusual saturation behavior of MR curves with respect to temperature is imputed to the superparamagneticlike spins at the interface, which leads to the high saturation field behavior of the magnetoresistance effect.

D. Temperature dependence of GMR in Fe/Ag

In well AFM coupled multilayers, it is believed^{4,17,26,29,30} that the GMR is generally enhanced with lowering temperature. On the one hand, it is because of the reduction of resistivity ρ_0 or the increase of the mean free path of conduction electrons. On the other hand, it is because of the increase of magnetic scattering ρ_M due to diminishing magnon excitations, which are thought to give rise to non-spin-dependent scattering. However, as seen from both Figs. 4 and 5, when the Ag thickness becomes thinner, the GMR exhibits such anomalous temperature dependence that the GMR at 1.5 K in a magnetic field of 60 kOe is even smaller than that at room temperature. This is very unusual.

The resistivity ρ and the net change in resistivity $\Delta\rho$ with respect to temperature for three representative samples with $t_{\text{Ag}}=10, 21, \text{ and } 32 \text{ \AA}$ are shown in Fig. 9, separately. In order to compare the temperature dependence of either $\Delta\rho/\rho$ or $\Delta\rho$ and ρ among different samples, they are normalized according to the values at 1.5 K. It is apparent that the ρ for all samples follows the usual temperature dependence rule, while the $\Delta\rho$ exhibits an anomalous temperature dependence. On the one hand, with decreasing temperature the ρ decreases, because the temperature-dependent scattering ρ_{s-d} caused by thermal excitation decreases. It also should be noted that with increasing Ag thickness, the reduction of ρ with respect to temperature becomes relatively weaker. This is closely associated with interfacial roughness, because for the sample with thinner Ag thickness it generally

possesses more significant interfacial roughness, and this may lead to the increase of the possibility for the occurrence of superparamagneticlike spins at interfacial regions in a large scale. In these regimes, thermal excitation may prevail at high temperature, but at low temperature it falls off, so that with decreasing temperature the resistivity may decay more prominently for a sample with a rougher interface. In the Fe/Cr superlattice,^{17,31} it has been found that with sharper interface, the resistivity is weakly dependent on temperature, while in sputtered superlattices,²⁶ which possess a rougher interface, it follows a power law that can be well described by thermal excitation of magnons as well as phonons.

On the other hand, the net change in resistivity due to related magnetic spin-dependent scattering for all samples displays such an unusual temperature dependence that at low temperature this change is diminished. Again, it seems to be inherently associated with interface roughness, and a rougher interface leads to a more pronounced decrease of $\Delta\rho$. In terms of the two-current model,⁷ if there is transfer of momentum between the two currents by spin-mixing scattering, the total resistivity is

$$\rho = \frac{\rho_{\uparrow}\rho_{\downarrow} + \rho_{\uparrow\downarrow}(\rho_{\uparrow} + \rho_{\downarrow})}{\rho_{\uparrow} + \rho_{\downarrow} + 4\rho_{\uparrow\downarrow}}, \quad (4)$$

where ρ_{\uparrow} and ρ_{\downarrow} denote the spin \uparrow and spin \downarrow resistivities, and $\rho_{\uparrow\downarrow}$ is the spin-mixing term. Both spin-flip and non-spin-flip scattering contribute to ρ_{σ} , but only spin-flip collisions give rise to $\rho_{\sigma\sigma'}$.

The general giant magnetoresistance, in a sense, just lies at the spin-mixing term caused by alternating magnetization or random arrangement of magnetization.³⁰ However, not only the scattering by alternating magnetization but also this scattering by superparamagneticlike spins and magnons, which is not necessarily spin dependent, gives rise to the spin-mixing term. At high temperature this spin-mixing term is inevitably enhanced due to thermal excitations. As discussed before, the thermal excitation of superparamagneticlike states, to some extent, could be suppressed in an external magnetic field, the contribution to the spin-mixing term from the superparamagneticlike spins may partially fall off, leading to the occurrence of an extra contribution to the magnetoresistance effect. This extra contribution may be greater at high temperature, where a lot of interfacial spins experience superparamagneticlike excitations. But at low temperature (1.5 K), the superparamagneticlike spins may significantly lock into the bulk layer, thus a large portion of contribution from suppression of superparamagneticlike spins may vanish and only the conventional magnetoresistance effect that associates with the spin-mixing term due to antiparallel magnetizations remains, so a relatively small $\Delta\rho$ is observed at 1.5 K. Generally, if the conventional GMR originating from spin mixing by alternating magnetization is moderate and the thermal excitation of superparamagneticlike spins is significant at a rougher interface region, the extra contribution to the GMR effect may be comparable to the general fraction of the GMR caused by AFM coupling. Therefore, with decrease of temperature the normal fraction of temper-

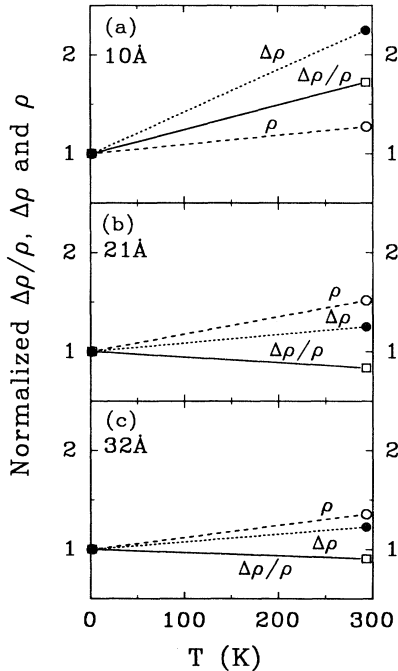


FIG. 9. The normalized temperature dependence of either $\Delta\rho/\rho$ or $\Delta\rho$ and ρ for samples $[\text{Fe}(10 \text{ \AA})/\text{Ag}(t_{\text{Ag}})]_{40}$ with t_{Ag} about (a) 10 \AA , (b) 21 \AA , and (c) 32 \AA . The lines are guide to eyes.

ature dependence of the general GMR may be masked by the extra contribution, and an anomalous temperature dependence of GMR may turn out. In our Fe/Ag films, it is true that the GMR arising from spin mixing due to the alternating magnetization is moderate. Moreover, assuming that the most responsible scattering for the GMR occurs at the interface between Fe and Ag layers, then the superparamagneticlike spins at the rougher interface make an important contribution to the GMR effect. Therefore, it is inevitable that the extra GMR emerges at high temperature, but falls off with reducing temperature because the superparamagneticlike spins are frozen and locked into the bulk layer. In addition, it should be noted that the extra contribution to the GMR (to some extent, e.g., the temperature dependence of $\Delta\rho$) is also dependent upon the spacer Ag thickness. As seen in Fig. 9, the thinner the Ag spacer, the stronger the temperature dependence of $\Delta\rho$. This is coherently associated with interfacial roughness. As showed in Sec. III, with a thinner Ag layer, the interface is rougher in general, which means that the possibility for formation of an assemblage of paramagnetic interfacial region increases. Consequently, thermal excitation of superparamagneticlike spins increases. So, the extra contributions to the GMR effect from the suppression of superparamagneticlike spins become more significant. As demonstrated in Figs. 4 and 5, owing to a relatively strong influence of the extra contribution, even the GMR ($\Delta\rho/\rho$) exhibits an anomaly for a sample with thinner Ag thickness, more precisely with a much rougher interface or more remarkable thermal excitations of superparamagneticlike spins.

V. CONCLUSIONS

The magnetoresistance with a maximum value of -7.3% in sputtered Fe/Ag multilayers has been reported. An oscillatory behavior of the GMR has been observed and the oscillation period is about 11 \AA . The GMR is believed to arise from spin-dependent scattering mainly occurring at interface and it depends on the interplay of interfacial superparamagneticlike spins and the AFM-coupled magnetization in neighboring Fe layers. The unusual temperature dependence of the saturation field, that with increasing temperature the MR curve shows a more significant high-field saturation behavior, has been interpreted in the light of interfacial superparamagneticlike spins. In addition, the anomaly of the temperature dependence of $\Delta\rho$, that the net change in resistivity induced by magnetic field is significantly smaller than that at room temperature, was attributed to suppression of the thermal excitations of superparamagneticlike spins at the interfacial layer. This suppression leads to an extra contribution to the GMR effect, but it may fall off at low temperature, resulting in the observed smaller GMR at 1.5 K .

ACKNOWLEDGMENTS

We wish to express many thanks to Professor Zhang Zong for his kind support and encouragement. This work was partially sponsored by Sanhuan Corporation of Chinese Academy of Sciences and State Key Laboratory of Advanced Metal Materials.

- ¹M. N. Baibich, J. M. Broto, A. Fert, F. Nguyen Van Dau, E. Petroff, P. Etienne, G. Creuzet, A. Friederich, and J. Chazelas, *Phys. Rev. Lett.* **61**, 2472 (1988).
- ²S. S. P. Parkin, N. More, and K. P. Roche, *Phys. Rev. Lett.* **64**, 2304 (1990).
- ³F. Petroff, A. Barthélemy, D. H. Mosca, D. K. Lottis, A. Fert, P. A. Schroeder, W. P. Pratt, Jr., and R. Loloee, *Phys. Rev. B* **44**, 5355 (1991).
- ⁴S. S. P. Parkin, R. Bhadra, and K. P. Roche, *Phys. Rev. Lett.* **66**, 2152 (1991).
- ⁵Y. Yafet, *J. Appl. Phys.* **61**, 4058 (1987); *Phys. Rev. B* **36**, 3948 (1987); R. Coehoorn, *ibid.* **44**, 9331 (1991).
- ⁶P. Bruno and C. Chappert, *Phys. Rev. Lett.* **67**, 1602 (1991).
- ⁷A. Fert and I. A. Campbell, *J. Phys. F* **6**, 849 (1976); I. A. Campbell and A. Fert, *Ferromagnetic Materials*, edited by E. P. Wohlfarth (North-Holland, Amsterdam, 1982), Vol. 3, p. 769.
- ⁸R. E. Camley and J. Barnas, *Phys. Rev. Lett.* **63**, 644 (1989); D. M. Edwards, J. Mathon, and R. B. Muniz, *IEEE Trans. Magn.* **MAG-27**, 3548 (1991); A. Barthélemy and A. Fert, *Phys. Rev. B* **43**, 13 124 (1991).
- ⁹P. M. Levy, S. Zhang, and A. Fert, *Phys. Rev. Lett.* **65**, 1643 (1990); S. Zhang, P. M. Levy, and A. Fert, *Phys. Rev. B* **45**, 8689 (1992); Hideo Hasegawa, *ibid.* **47**, 15 073 (1993); A. Vedyayev, C. Cowache, N. Ryzhanova, and B. Dieny, *J. Phys. Condens. Matter* **5**, 8289 (1993).
- ¹⁰A. E. Berkowitz, J. R. Mitchell, M. J. Carey, A. P. Young, S. Zhang, F. E. Spada, F. T. Parker, A. Hutten, and G. Thomas, *Phys. Rev. Lett.* **68**, 3745 (1992); J. Q. Xiao, J. S. Jiang, and C. L. Chien, *ibid.* **68**, 3749 (1992).
- ¹¹Z. Celinski and B. Heinrich, *J. Magn. Magn. Mater.* **99**, L25 (1991); A. Fuss, S. Demokritov, P. Grunberg, and W. Zinn, *ibid.* **103**, L221 (1992).
- ¹²J. Unguris, R. J. Celotta, and D. T. Pierce, *J. Magn. Magn. Mater.* **127**, 205 (1993).
- ¹³Z. Celinski, B. Heinrich, and J. F. Cochran, *J. Appl. Phys.* **73**, 5966 (1993).
- ¹⁴G. Xiao, J. Q. Wang, and P. Xiong, *Appl. Phys. Lett.* **62**, 420 (1993).
- ¹⁵M. B. Stearns, C. H. Lee, and T. L. Groy, *Phys. Rev. B* **40**, 8256 (1989); F. J. Lamelas, H. David, and Roy Clarke, *ibid.* **43**, 12 296 (1991).
- ¹⁶J. Q. Xiao, A. Gavrin, Gang Xiao, J. R. Childress, W. A. Bryden, C. L. Chien, and A. S. Edelstein, *J. Appl. Phys.* **67**, 5388 (1990).
- ¹⁷A. Barthélemy, A. Fert, M. N. Baibich, S. Hadjoudj, F. Petroff, P. Etienne, R. Cabanel, S. Lequien, F. Nguyen Van Dau, and G. Creuzet, *J. Appl. Phys.* **67**, 5908 (1990).
- ¹⁸M. A. Howson, B. J. Hickey, J. Xu, and D. Greig, *Phys. Rev. B* **48**, 1322 (1993); K. Le Dang, P. Veillet, E. Velu, S. S. P. Parkin, and C. Chappert, *Appl. Phys. Lett.* **63**, 108 (1993).
- ¹⁹A. Schreyer, and K. Brohl, J. F. Ankner, C. F. Majkrzak, Th. Zeidler, P. Bodeker, N. Metoki, and H. Zabel, *Phys. Rev. B* **47**, 15 334 (1993).

- ²⁰E. E. Fullerton, D. M. Kelly, J. Guimpel, I. K. Schuller, and Y. Bruynseraede, *Phys. Rev. Lett.* **68**, 859 (1992).
- ²¹S. S. P. Parkin, *Phys. Rev. Lett.* **71**, 1641 (1993).
- ²²F. Tsui, B. Chen, D. Barlett, R. Clarke, and C. Uher, *Phys. Rev. Lett.* **72**, 740 (1994).
- ²³D. Barlett, F. Tsui, D. Glick, L. Lauhon, T. Mandrekar, C. Uher, and R. Clarke, *Phys. Rev. B* **49**, 1521 (1994).
- ²⁴B. Dieny, P. Humbert, V. S. Speriosu, S. Metin, B. A. Gurney, P. Baumgart, and H. Lefakis, *Phys. Rev. B* **45**, 806 (1992).
- ²⁵J. C. Slonczewski, *J. Appl. Phys.* **73**, 5957 (1993).
- ²⁶J. E. Mattson, M. E. Brubaker, C. H. Sowers, M. Conover, Z. Qiu, and S. D. Bader, *Phys. Rev. B* **44**, 9378 (1991).
- ²⁷S. S. P. Parkin, *Appl. Phys. Lett.* **61**, 1358 (1992).
- ²⁸R. Q. Hood, L. M. Falicov, and D. R. Penn, *Phys. Rev. B* **49**, 368 (1994).
- ²⁹M. A. M. Gijs, S. K. J. Lenczowski, and J. B. Giesbers, *Phys. Rev. Lett.* **70**, 3343 (1993).
- ³⁰S. Zhang and P. M. Levy, *Phys. Rev. B* **43**, 11 048 (1991).
- ³¹F. Petroff, A. Barthélémy, A. Hamzic, A. Fert, P. Etienne, S. Lequien, and G. Creuzet, *J. Magn. Magn. Mater.* **93**, 95 (1991).

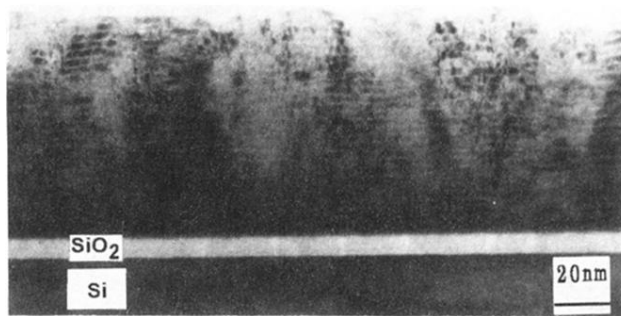


FIG. 3. The cross-section TEM image of sample $[\text{Fe}(10 \text{ \AA})/\text{Ag}(21 \text{ \AA})]_{40}$. The white layer corresponds to Fe layer, and the dark layer to Ag layer.